Han X, et al., J Cytol Tissue Biol 2017, 4: 015
DOI: 10.24966/CTB-9107/100015

HSOA Journal of Cytology and Tissue Biology

Research Article

Ant-Inflammatory Activity of Spearmint (*Mentha spicata*) Essential Oil in Human Dermal Fibroblasts

Xuesheng Han*, Cody Beaumont and Tory L Parker*

dōTERRA International, LLC, Pleasant Grove, UT, USA

Abstract

The use of Spearmint (*Mentha spicata*) Essential Oil (SEO) in skin care products has become popular. In this study, we evaluated the impact of a commercially available SEO on 17 protein biomarkers that perform critical functions in inflammation and tissue remodeling in a validated human dermal fibroblast system, which was designed to model the pathology of chronic inflammation. The impact of SEO on genome-wide gene expression was also evaluated. SEO showed robust antiproliferative effects in diseased human skin cells and significantly inhibited the increased production of two pro-inflammatory biomarkers Vascular Cell Adhesion Molecule-1 (VCAM-1) and interferon-inducible T-cell α Chemoattractant (I-TAC). In contrast, SEO significantly increased the levels of Monocyte Chemoattractant Protein-1 (MCP-1), Epidermal Growth Factor Receptor (EGFR), Matrix Metalloproteinase-1 (MMP-1) and Tissue Inhibitor of Metalloproteinase-1 (TIMP-1). SEO significantly modulated global gene expression and altered signaling pathways, many of which are critical in the inflammatory and tissue remodeling processes. Further analysis showed that the gene expression data obtained were consistent with the observed anti-inflammatory and tissue remodeling effects of SEO. This study provided the first evidence of SEO 's anti-inflammatory activity in human dermal fibroblasts, which suggested that SEO might be a promising candidate for anti-inflammatory skincare products.

Keywords: Antiproliferation; Genome-wide gene expression; Inflammation; *Mentha spicata*; Skin health; Spearmint essential oil

Introduction

Spearmint (*Mentha spicata*) Essential Oil (SEO) is rich in carvone and limonene and has a refreshing aroma. In comparison with peppermint essential oil, SEO is perceived to be a milder option for topical application in individuals with sensitive skin. This could be one of the reasons for the increased popularity of SEO in skin care, beauty and healthcare products. Studies in various models have demonstrated its therapeutic potential, which include antiproliferative, antibacterial, antifungal, anticonvulsant and antiemetic activities [1-7]. However, studies on the effects of SEO in human skin cells are scarce. Although the anti-inflammatory properties of limonene, a major active component of SEO, have been demonstrated in both pre-clinical and clinical models; to our knowledge, no studies have been conducted to evaluate the anti-inflammatory activity of SEO in human dermal fibroblasts.

We investigated the biological activity of a commercially available SEO in a validated human dermal fibroblast cell culture line designed to model the pathology of chronic inflammation [8,9]. We analyzed the impact of SEO on 17 important protein biomarkers closely related to the inflammatory and tissue remodeling pathways. We also studied the regulatory effect of SEO on genome-wide gene expression.

Materials and Methods

All experiments were conducted in a Biologically Multiplexed Activity Profiling (Bio MAP) system HDF3CGF, a cell culture system of human dermal fibroblasts designed to model chronic inflammation and fibrosis in a robust and reproducible way. The system consists of three components: cells, stimuli to create the disease environment, and a set of biomarker (protein) readouts to examine how the treatments affect the disease environment [10]. The methodologies used in this study were essentially the same as those previously described [10-12]. The study was approved before commencement and followed the guidelines for human subject research under the regulations (45 CFR Part 46) of the US Department of health and human services.

Cell cultures

Primary human neonatal foreskin fibroblasts were prepared as previously described and plated in low-serum conditions for 24 h before stimulation with a mixture of Interleukin (IL)-1β [9], Tumor Necrosis Factor (TNF)-α, Interferon (IFN)-γ, basic Fibroblast Growth Factor (bFGF), Epidermal Growth Factor (EGF), and Platelet-Derived Growth Factor (PDGF). The cell culture and stimulation conditions for the HDF3CGF assays have been described in detail elsewhere and the assays were performed in a 96 well format [9,13].

Protein based readouts

An Enzyme Linked Immunosorbent Assay (ELISA) was used to measure the biomarker levels of cell associated and cell membrane targets. The soluble factors from the supernatants were quantified by using homogeneous time resolved fluorescence detection, bead based multiplex immunoassay, or capture ELISA. The overt adverse effects of the test agents on cell proliferation and viability (i.e., cytotoxicity) were measured by using the Sulforhodamine B (SRB) assay. For proliferation assays, the cells were cultured and then assayed after 72 h, which is optimal for the HDF3CGF system the detailed information has been described elsewhere [9]. The measurements were performed in triplicate and a glossary of the biomarkers used in this study is provided in supplementary table S1.

The quantitative biomarker data were presented as the mean $\log_{10}$ relative expression level (compared with the respective mean vehicle

***Corresponding authors:** Xuesheng Han, dōTERRA International, LLC, Pleasant Grove, USA, Tel: +1 801 4377976; E-mail: lhan@doterra.com

Tory L Parker, dōTERRA International, LLC, Pleasant Grove, USA, Tel: +1 801 437 7957; E-mail: tparker@doterra.com

Citation: Han X, Beaumont C, Parker TL (2017) Anti-Inflammatory Activity of Spearmint (Mentha spicata) Essential Oil in Human Dermal Fibroblasts. J Cytol Tissue Biol 4: 015.

Received: March 01, 2017; **Accepted:** July 26, 2017; **Published:** August 07, 2017

control value) ± Standard Deviation (SD) of triplicate measurements. The differences in biomarker levels between the SEO and vehicle treated cultures were tested for significance with an unpaired Student's *t*-test. A p-value < 0.05, outside of the significance envelope, with an effect size of at least 10% (more than 0.05 $\log_{10}$ ratio units), was considered statistically significant.

RNA isolation

Total RNA was isolated from the cell lysates using the Zymo Quick-RNA MiniPrep kit (Zymo Research Corporation, Irvine, CA, USA) in accordance with the manufacturer's instructions. The RNA concentration was measured using a NanoDrop ND-2000 (Thermo Fisher Scientific, Waltham, MA, USA) and the RNA quality was assessed by using a Bioanalyzer 2100 (Agilent Technologies, Santa Clara, CA, USA) and an Agilent RNA 6000 Nano Kit. All samples had an A260/A280 ratio between 1.9 and 2.1 and an RNA integrity number score greater than 8.0.

Microarray analysis for genome-wide gene expression

A solution of 0.011% (v/v) SEO was tested for its effect on the expression of 21,224 genes in the HDF3CGF system after a 24-h treatment period. The samples for microarray analysis were processed by Asuragen, Inc. (Austin, TX, USA) in accordance with the company's standard operating procedures. Biotin-labeled cRNA was prepared from 200 ng of total RNA with an Illumina total Prep RNA Amplification kit (Thermo Fisher Scientific) and one round of amplification. The cRNA yields were quantified via ultraviolet spectroscopy, and the distribution of transcript sizes was assessed using the Agilent Bioanalyzer 2100. Labeled cRNA (750 ng) was used to probe Illumina Human HT-12 v4 Expression Bead Chips (Illumina, Inc., San Diego, CA, USA). Hybridizing, washing, staining with streptavidin-conjugated cyanine-3, and scanning of the Illumina arrays were performed in accordance with the manufacturer's instructions. Illumina bead scan software was used to produce the data files for each array and raw data were extracted using the Illumina bead studio software.

The raw data were uploaded into and analyzed for quality control metrics using the bead array package [13,14]. The data were normalized using quantile normalization and then re-annotated and filtered to remove probes that were non-specific or mapped to intronic or intragenic regions [15,16]. The remaining probe sets comprised the data set for the rest of the analysis. Fold-change expression for each value was calculated as the $\log_2$ ratio of SEO to the vehicle control. These fold change values were uploaded into the Ingenuity Pathway Analysis (IPA, Qiagen, Redwood City, CA, USA) to generate the networks and pathway analyses.

Reagents

SEO (provided by dōTERRA International LLC, Pleasant Grove, UT, USA) was diluted in Dimethyl Sulfoxide (DMSO) to 8× the specified concentration (the final DMSO concentration in the culture media was no more than 0.1% [v/v]); 25 µL of each 8× solution was added to the cell culture to give a final volume of 200 µL DMSO (0.1%) served as the vehicle control.

The chemical composition of the oil was analyzed using Gas Chromatography-Mass Spectrometry (GC-MS). Detailed methods of GC-MS have been previously described [12]. GC-MS analysis of SEO indicated that its major chemical constitutes (i.e., >5%) are carvone (68%) and limonene (19%). The GC-MS chromatography of SEO has been included in supplementary figure 1.

Results and Discussion

Bioactivity profile of SEO in the human dermal fibroblast system HDF3CGF

We analyzed the activity of SEO in a dermal fibroblast cell system, HDF3CGF, which features the microenvironment of inflamed human skin cells with an already boosted immune response and inflammation level. Initially, four concentrations of SEO (0.011, 0.0037, 0.0012 and 0.00041%, v/v) were tested for biological activity; none of the concentrations showed clear cytotoxicity. The highest tested concentration of 0.011% was selected for further study. A key biomarker modulation activity was inferred if the biomarker values in the treated cells were significantly different ($p<0.05$) from those of the vehicle controls, with an effect size of at least 10% (more than 0.05 log ratio units; Figure 1).

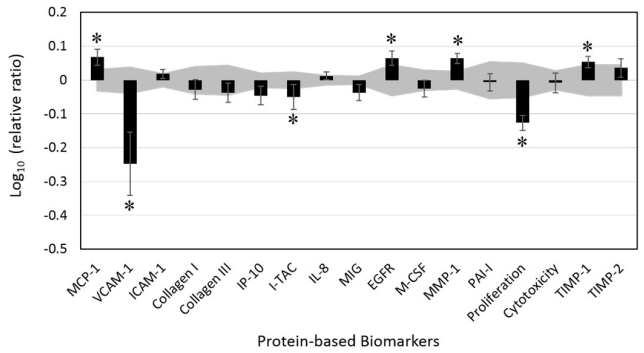

Figure 1: Bioactivity profile of spearmint essential oil (SEO, 0.011% v/v) in a human dermal fibroblast system (HDF3CGF).

X-axis denotes protein-based biomarker readouts. Y-axis denotes the relative expression levels of biomarkers compared with the vehicle control values in the log form. The vehicle control values are marked in gray with a 95% confidence level.

*indicates a biomarker designated with "key activity"; the biomarker value for the treated cells was significantly different ($p<0.05$) from that of the vehicle control at the tested concentration, with an effect size of at least 10% (more than 0.05 log ratio units). MCP-1- Monocyte Chemoattractant Protein 1; VCAM-1 - Vascular Cell Adhesion Molecule 1; ICAM-1 - Intracellular Cell Adhesion Molecule 1; IP-10 - Interferon Gamma-Induced Protein 10; I-TAC - Interferon-inducible T-cell Alpha Chemoattractant; IL-8 - Interleukin 8; MIG - Monokine Induced by Gamma Interferon; EGFR - Epidermal Growth Factor Receptor; M-CSF - Macrophage Colony-Stimulating Factor; MMP-1 - Matrix Metalloproteinase 1; PAI-1 - Plasminogen Activator Inhibitor 1; SRB - Sulforhodamine B; TIMP - Tissue Inhibitors of Metalloproteinase

Overall, SEO demonstrated diverse effects on multiple protein molecules, including significant antiproliferative activity in dermal fibroblast cells. In addition, SEO significantly suppressed the increased production of two pro-inflammatory biomarkers, Vascular Cell Adhesion Molecule-1 (VCAM-1) and Interferon-inducible T-cell Alpha Chemoattractant (I-TAC). In contrast, SEO significantly increased the level of Monocyte Chemoattractant Protein 1 (MCP-1), which is also a pro-inflammatory chemokine. The important biomarkers related to tissue remodeling, namely Epidermal Growth Factor Receptor (EGFR), Matrix Metalloproteinase-1 (MMP-1) and Tissue Inhibitor of Metalloproteinase-1 (TIMP-1) were also significantly increased by SEO. SEO had no significant effect on the other biomarkers tested in the experimental system.

Zhao et al., reported that SEO reduced pulmonary inflammation in rats with chronic obstructive pulmonary disease [17]. de Sousa et al., observed the spasmolytic activity of carvone and limonene, which can assist proper respiratory and cardiovascular functioning [18]. A recent human study demonstrated the beneficial effects of SEO on lung function and exercise performance [19], which may be at least

partially attributed to its anti-inflammatory and spasmolytic features recently showed that SEO rich in carvone (85.4%) exhibited antiproliferative activity in cancer cells [1].

Carvone and limonene were found to modulate immune response in BALB/c mice [20]. Studies on carvone derivatives also demonstrated their anti-inflammatory potential [18]. de Sousa et al. reported that orally administered hydroxydihydrocarvone exerted anti-inflammatory effects in rats and mice [21,22]. Marques et al. studied the anti-inflammatory activity of cyane-carvone, a synthetic derivative of carvone, and found that it significantly decreased IL-1β and TNF-α levels and significantly inhibited paw edema in mice [22].

Several studies of limonene showed that it demonstrated anti-inflammatory potential in a variety of disease models, possibly through the suppression of pro-inflammatory cytokines [23,24], p38 mitogen activated protein kinase, nuclear factor-κB, c-Jun N-terminal kinase , and extracellular signal-regulated kinase [25-28]. Notably, Rufino et al. observed that limonene increased the gene expression of TIMP-1 and decreased the expression of MMP-1 in a mouse model of osteoarthritis [23]. The results of the current study showed that SEO significantly increased the protein levels of TIMP-1 and MMP-1 in a human skin disease model.

Studies have also shown evidence that carvone and limonene act as transdermal permeation enhancers [29]. Limonene has been found to promote skin repair and inhibit skin tumorigenesis [30,28]. Both these properties are partly attributable to its anti-inflammatory activity. These features may further contribute to the beneficial effects of SEO on skin health.

Effects of SEO on genome-wide gene expression in the HDF3CGF system

We studied the effects of 0.011% SEO (The highest tested concentration that was not cytotoxic to the cells) on the RNA expression of 21,224 genes in the HDF3CGF system. The results show that SEO significantly modulated global gene expression; many genes were up-regulated or down regulated (Table S2). Among the 200 most affected genes ($\log_2$ [expression fold change ratio relative to vehicle control] ≥ |1.5|) by SEO, the majority (148 of 200 genes) were significantly down regulated and the rest were up regulated. A cross comparison of protein and gene expression results showed that SEO significantly inhibited both the protein and gene expression of *VCAM-1* and *I-TAC*.

Further, IPA studies indicated that the pattern of SEO bioactivity matched multiple canonical pathways listed in the literature-validated signaling pathway database (Figure 2). Many of these pathways play critical roles in the processes of inflammation, tissue remodeling and immune modulation. The overall inhibitory effect of SEO on these genes and signaling pathways appeared consistent with its observed anti-inflammatory properties; the Supplementary Material contains more detailed information.

Collectively, these data showed that SEO, of which the main components are carvone and limonene, had significant antiproliferative and anti-inflammatory activities in human dermal fibroblasts. In addition, these findings suggested that SEO might be able to modulate immune responses during the wound healing process and promote improved wound healing. The results of the current study were consistent with those of existing studies, which indicated the therapeutic potential of SEO as an anti-inflammatory candidate for skin care products. Further research into its biological mechanism of action in specific disease models, as well as its clinical efficacy and safety, is recommended.

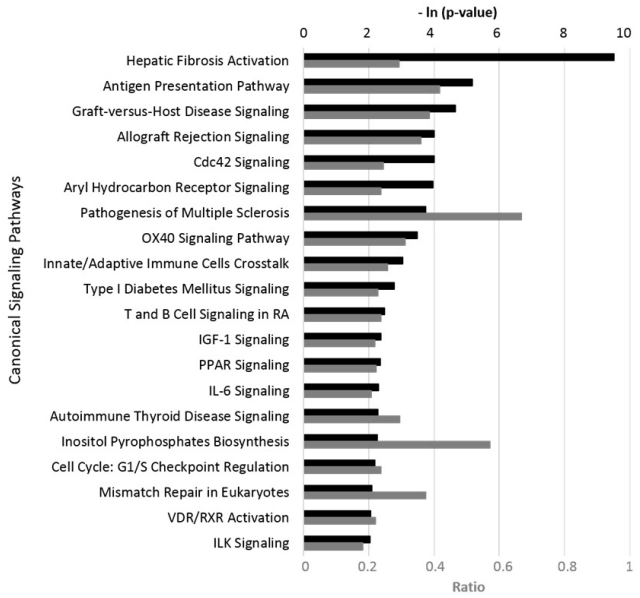

Figure 2: Top 20 canonical pathways matching the bioactivity profile of Spearmint Essential Oil (SEO, 0.011% v/v) for gene expression in the human dermal fibroblast system (HDF3CGF), produced via ingenuity pathway analysis.

The p-value is calculated using right-tailed Fisher's Exact Test. It indicates how likely the observed association between a specific pathway and the dataset would be if it resulted from random chance only. The smaller the p-value (that is, the bigger the - ln [p-value], indicated by the black bars) of a pathway, the greater the match with the bioactivity of SEO. The ratio, indicated by the gray bar, was calculated by taking the number of genes from the SEO dataset that participate in a canonical pathway and dividing it by the total number of genes in that pathway.

Cdc42 - cell division control protein 42 homolog; OX40 - tumor necrosis factor receptor super family, member 4; RA- Rheumatoid Arthritis; IGF- 1 - Insulin-Like Growth Factor 1; PPAR - Peroxisome Proliferator-Activated Receptors; VDR - Vitamin D Receptor; RXR - Retinoid X Receptor; ILK - Integrin-Linked Kinase.

Conclusion

To our knowledge, this is the first study to evaluate the biological activity of SEO in pre-inflamed human dermal fibroblast cells. SEO showed significant antiproliferative activity through the inhibition of *VCAM-1* and I-TAC levels and the increased expression of MCP-1, EGFR, MMP-1 and TIMP-1. Genome-wide gene expression analysis demonstrated that SEO exerted a robust and diverse impact on the expression of many genes. Many of the genes and pathways highly affected by SEO were critically involved in the inflammatory and tissue remodeling processes. These results were consistent with those of other studies that reported the anti-inflammatory and wound healing potential of SEO. Although the clinical efficacy and safety of SEO administration are still undetermined, our study indicated that SEO was a promising candidate for use in anti-inflammatory skin products.

Acknowledgment

This study was funded by dōTERRA (Pleasant Grove, UT, USA) and conducted at DiscoverX (Fremont, CA, USA). Author contributions: Xuesheng Han interpreted the data and drafted the manuscript. Cody Beaumont developed and conducted the GC-MS assays. Tory Parker oversaw the study design, methodology, and study agent and model selection. All authors reviewed and approved the final manuscript.

Conflicts of Interest

Xuesheng Han, Cody Beaumont and Tory Parker are employees of dōTERRA, the manufacturer of the study agent (SEO).

References

1. Fitsiou E, Mitropoulou G, Spyridopoulou K, Tiptiri-Kourpeti A, Vamvakias M, et al. (2016) Phytochemical profile and evaluation of the biological activities of essential oils derived from the greek aromatic plant species Ocimum basilicum, *Mentha spicata*, *Pimpinella anisum* and *Fortunella margarita*. Molecules 21.
2. Hussain AI, Anwar F, Nigam PS, Ashraf M, Gilani AH (2010) Seasonal variation in content, chemical composition and antimicrobial and cytotoxic activities of essential oils from four *Mentha* species. Journal of the Science of Food and Agriculture 90: 1827-1836.
3. Shahbazi Y (2015) Chemical Composition and *In Vitro* Antibacterial Activity of *Mentha spicata* Essential Oil against Common Food-Borne Pathogenic Bacteria. Journal of Pathogens 916305.
4. Houicher A, Hechachna H, Teldji H, Ozogul F (2016) *In Vitro* Study of the Antifungal Activity of Essential Oils Obtained from *Mentha spicata*, *Thymus vulgaris*, and *Laurus nobilis*. Recent Pat Food Nutr Agric 8: 99-106.
5. Nardoni S, Giovanelli S, Pistelli L, Mugnaini L, Profili G, et al. (2015) *In Vitro* Activity of Twenty Commercially Available, Plant-Derived Essential Oils against Selected Dermatophyte Species. Nat Prod Commun 10: 1473-1478.
6. Koutroumanidou E, Kimbaris A, Kortsaris A, Bezirtzoglo E, Polissio M, et al. (2013) Increased seizure latency and decreased severity of pentylenetetrazol-induced seizures in mice after essential oil administration. Epilepsy Research and Treatment 532657.
7. Tayarani-Najaran Z, Talasaz-Firoozi E, Nasiri R, Jalali N, Hassanzadeh MK (2013) Antiemetic activity of volatile oil from *Mentha spicata* and *Mentha × Piperita* in chemotherapy-induced nausea and vomiting. Ecancermedicalscience 7: 290.
8. Kunkel EJ, Dea M, Ebens A, Hytopoulos E, Melrose J, et al. (2004) An integrative biology approach for analysis of drug action in models of human vascular inflammation. FASEB J 18: 1279-1281.
9. Bergamini G, Bell K, Shimamura S, Werner T, Cansfield A, et al. (2012) A selective inhibitor reveals PI3Kγ dependence of T_H17 cell differentiation. Nature Chemical Biology 8: 576-582.
10. Berg EL, Yang J, Melrose J, Nguyen D, Privat S, et al. (2010) Chemical target and pathway toxicity mechanisms defined in primary human cell systems. Journal of Pharmacological and Toxicological Methods 61: 3-15.
11. Han X, Parker TL (2017) Anti-inflammatory, tissue remodeling, immunomodulatory, and anticancer activities of oregano (*Origanum vulgare*) essential oil in a human skin disease model. Biochimie Open 4: 73-77.
12. Han X, Beaumont C, Stevens N (2017) Chemical composition analysis and *in vitro* biological activities of ten essential oils in human skin cells. Biochimie Open 5: 1-7.
13. R Development Core Team (2011) *R: A* Language and Environment for Statistical Computing. The R Foundation for Statistical Computing, Vienna, Austria.
14. Dunning MJ, Smith ML, Ritchie ME, Tavaré S (2007) beadarray: R classes and methods for Illumina bead-based data. Bioinformatics 23: 2183-2184.
15. Bolstad BM, Irizarry RA, Astrand M, Speed TP (2003) A comparison of normalization methods for high density oligonucleotide array data based on variance and bias. Bioinformatics 19: 185-193.
16. Barbosa-Morais NL, Dunning MJ, Samarajiwa SA, Darot JFJ, Ritchie ME, et al. (2010) A re-annotation pipeline for Illumina BeadArrays: improving the interpretation of gene expression data. Nucleic Acids Res 38: 17.
17. Zhao CZ, Wang Y, Tang FD, Zhao XJ, Xu QP, et al. (2008) [Effect of Spearmint oil on inflammation, oxidative alteration and Nrf2 expression in lung tissue of COPD rats]. Zhejiang Da Xue Xue Bao Yi Xue Ban 37: 357-363.
18. de Sousa DP, Mesquita RF, de Araújo Ribeiro LA, de Lima JT (2015) Spasmolytic Activity of Carvone and Limonene Enantiomers. Nat Prod Commun 10: 1893-1896.
19. Jaradat NA, Al Zabadi H, Rahhal B, Hussein AM, Mahmoud JS, et al. (2016) The effect of inhalation of Citrus sinensis flowers and *Mentha spicata* leave essential oils on lung function and exercise performance: a quasi-experimental uncontrolled before-and-after study. J Int Soc Sports Nutr 13: 36.
20. Raphael TJ, Kuttan G (2003) Immunomodulatory activity of naturally occurring monoterpenes carvone, limonene, and perillic acid. Immunopharmacol Immunotoxicol 25: 285-294.
21. de Sousa DP, Camargo EA, Oliveira FS, de Almeida RN (2010) Anti-inflammatory activity of hydroxydihydrocarvone. Z Naturforsch C 65: 543-550.
22. Marques TH, Marques ML, Medeiros JV, Silva RO, dos Reis Barbosa AL, et al. (2014) Cyane-carvone, a synthetic derivative of carvone, inhibits inflammatory response by reducing cytokine production and oxidative stress and shows antinociceptive effect in mice. Inflammation 37: 966-977.
23. Rufino AT, Ribeiro M, Sousa C, Judas F, Salgueiro L, et al. (2015) Evaluation of the anti-inflammatory, anti-catabolic and pro-anabolic effects of E-caryophyllene, myrcene and limonene in a cell model of osteoarthritis. Eur J Pharmacol 750: 141-150.
24. Yoon WJ, Lee NH, Hyun CG (2010) Limonene suppresses lipopolysaccharide-induced production of nitric oxide, prostaglandin E2, and pro-inflammatory cytokines in RAW 264.7 macrophages. J Oleo Sci 59: 415-421.
25. Chi G, Wei M, Xie X, Soromou LW, Liu F, et al. (2013) Suppression of MAPK and NF-κB pathways by limonene contributes to attenuation of lipopolysaccharide-induced inflammatory responses in acute lung injury. Inflammation 36: 501-511.
26. Rehman MU, Tahir M, Khan AQ, Khan R, Oday-O-Hamiza, et al. (2014) D-limonene suppresses doxorubicin-induced oxidative stress and inflammation via repression of COX-2, iNOS, and NFκB in kidneys of Wistar rats. Exp Biol Med (Maywood) 239: 465-476.
27. Kim K-N, Ko Y-J, Yang H-M, Ham Y-M, Roh SW, et al. (2013) Anti-inflammatory effect of essential oil and its constituents from fingered citron (Citrus medica L. var. *sarcodactylis*) through blocking JNK, ERK and NF-κB signaling pathways in LPS-activated RAW 264.7 cells. Food and Chemical Toxicology 57: 126-131.
28. Chaudhary SC, Siddiqui MS, Athar M, Alam MS (2012) D-Limonene modulates inflammation, oxidative stress and Ras-ERK pathway to inhibit murine skin tumorigenesis. Human & Experimental Toxicology 31: 798-811.
29. Krishnaiah YS, Raju V, Shiva Kumar M, Rama B, Raghumurthy V, et al. (2008) Studies on optimizing in vitro transdermal permeation of ondansetron hydrochloride using nerodilol, carvone, and limonene as penetration enhancers. Pharm Dev Technol 13: 177-185.
30. d'Alessio PA, Mirshahi M, Bisson JF, Bene MC (2014) Skin repair properties of d-Limonene and perillyl alcohol in murine models. Antiinflamm Antiallergy Agents Med Chem 13: 29-35.

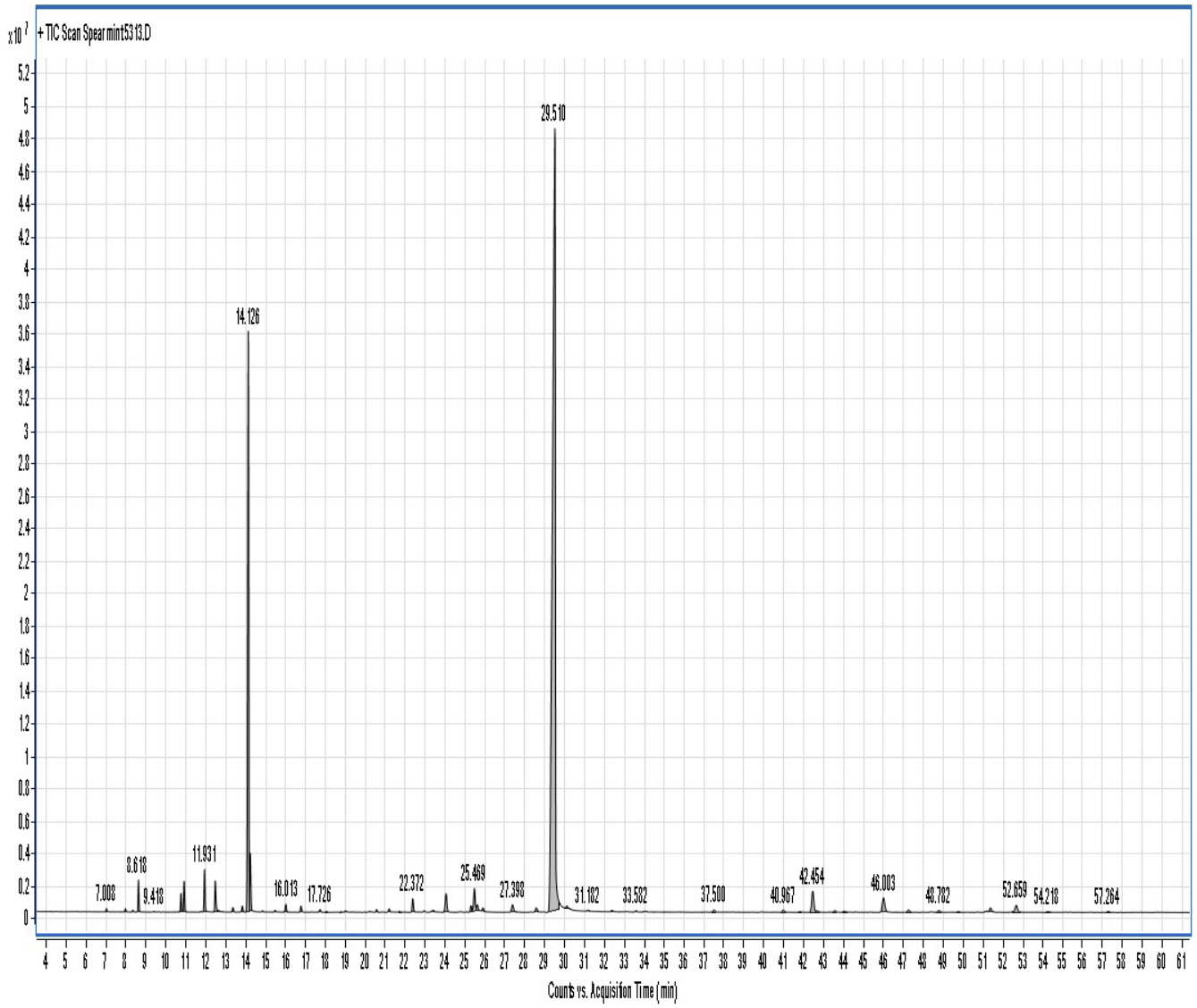

Figure 1: The chromatography of spearmint essential oil analyzed by GC-MS.

Readout	Description
CCL2/MCP-1	MCP-1 system is a chemokine that mediates recruitment of monocytes and T cells into sites of inflammation. MCP-1 is categorized as an inflammation related activity in the HDF3CGF system modeling Th1 inflammation involved in wound healing and matrix remodeling.
CD106/VCAM-1	VCAM-1 is a cell adhesion molecule that mediates adhesion of monocytes and T cells to endothelial cells. VCAM-1 is categorized as an inflammation-related activity.
CD54/ICAM-1	ICAM-1 is a cell adhesion molecule that mediates leukocyte-endothelial cell adhesion and leukocyte recruitment. ICAM-1 is categorized as an inflammation-related activity.
Collagen I	Collagen I is involved in tissue remodeling and fibrosis, and is the most common fibrillar collagen that is found in skin, bone, tendons and other connective tissues. Collagen I is categorized as a tissue remodeling-related activity.
Collagen III	Collagen III is an extracellular matrix protein and fibrillar collagen found in extensible connective tissues (skin, lung and vascular system) and is involved in cell adhesion, cell migration, tissue remodeling. Collagen III is categorized as a tissue remodeling-related activity.
CXCL10/IP-10	IP-10 is a chemokine that mediates T cell, monocyte and dendritic cell chemotaxis. IP-10 is categorized as an inflammation-related activity.
CXCL11/I-TAC	I-TAC is a chemokine that mediates T cell and monocyte chemotaxis. I-TAC is categorized as an inflammation-related activity.
CXCL8/IL-8	IL-8 is a chemokine that mediates neutrophil recruitment into acute inflammatory sites. IL-8 is categorized as an inflammation-related activity.
CXCL9/MIG	MIG is a chemokine that mediates T cell recruitment. MIG is categorized as an inflammation-related activity.
EGFR	EGFR is a cell surface receptor for epidermal growth factor involved in cell proliferation during development as well as tumor growth. EGFR is involved in Epithelial cell proliferation, epithelial cell differentiation keratinocyte proliferation, tissue remodeling. EGFR is categorized as a tissue remodeling-related activity.

M-CSF	M-CSF is a secreted and cell surface cytokine that mediates macrophage differentiation. M-CSF is categorized as animmune modulation-related activity.
MMP-1	MMP-1 is an interstitial collagenase that degrades collagens I, II and III and is involved in the process of tissue remodeling. MMP-1 is categorized as a tissue remodeling-related activity.
PAI-I	PAI-I is a serine proteinase inhibitor and inhibitor of tissue Plasminogen Activator (tPA) and urokinase (uPA) and is involved in tissue remodeling and fibrinolysis. PAI-I is categorized as a tissue remodeling-related activity.
Proliferation 72hr	Proliferation 72hr in the HDF3CGF system is a measure of dermal fibroblast proliferation which is important to the process of wound healing and fibrosis.
SRB	SRB is a measure of the total protein content of dermal fibroblasts. Cell viability of adherent cells is measured by Sulforhodamine B (SRB) staining, a method that determines cell density by measuring total protein content of test wells.
TIMP-1	TIMP-1 is a tissue inhibitor of Matrix Metalloprotease-7 (MMP-7) and other MMPs, and is involved in tissue remodeling, angiogenesis and fibrosis. TIMP-1 is categorized as a tissue remodeling-related activity.
TIMP-2	TIMP-2 is a tissue inhibitor of matrix metalloproteases and is involved in tissue remodeling, angiogenesis and fibrosis. TIMP-2 is categorized as a tissue remodeling-related activity.

Table 1: Glossary of biomarkers of the human dermal fibroblast system (HDF3CGF) used in the study.

Illumina Gene ID	Fold Change in Log_2 form	Definition
TFRC	2.69	*Homo sapiens* Transferrin Receptor (p90, CD71) (TFRC), mRNA.
AKR1C4	2.33	*Homo sapiens* Aldo-Keto Reductase family 1, member C4 (chlordecone reductase; 3-alpha hydroxysteroid dehydrogenase, type I; dihydrodiol dehydrogenase 4) (AKR1C4), mRNA.
GSTA2	2.13	*Homo sapiens* Glutathione S-Transferase A2 (GSTA2), mRNA.
CDCA7	2.05	*Homo sapiens* Cell Division Cycle Associated 7 (CDCA7), transcript variant 1, mRNA.
TSPAN13	1.96	*Homo sapiens* Tetraspanin 13 (TSPAN13), mRNA.
HS.527671	1.82	UI-CF-FN0-age-p-21-18-UI.r18 UI-CF-FN0 *Homo sapiens* cDNA clone UI-CF-FN0-age-p-21-18-UI 5, mRNA sequence
MIR1914	1.81	*Homo sapiens* microRNA 1914 (MIR1914), microRNA.
HNRNPA1	1.80	*Homo sapiens* Heterogeneous Nuclear Ribonucleoprotein A1 (HNRNPA1), transcript variant 2, mRNA.
LOC650922	1.79	PREDICTED: *Homo sapiens* hypothetical LOC650922 (LOC650922), mRNA.
HS.544326	1.74	hd38d03.x1 Soares_NFL_T_GBC_S1 *Homo sapiens* cDNA clone IMAGE:2911781 3, mRNA sequence.
HNRPH1	1.74	*Homo sapiens* Heterogeneous Nuclear Ribonucleoprotein H1 (H) (HNRPH1), mRNA.
FGF6	1.71	*Homo sapiens* Fibroblast Growth Factor 6 (FGF6), mRNA.
HS.374832	1.71	DA086964 BRACE2 *Homo sapiens* cDNA clone BRACE2041741 5, mRNA sequence
LOC100101266	1.70	*Homo sapiens* hepatitis A virus cellular receptor 1 pseudogene (LOC100101266), non-coding RNA.
GTF2I	1.69	*Homo sapiens* General Transcription Factor II, i (GTF2I), transcript variant 1, mRNA.
LOC731042	1.69	PREDICTED: *Homo sapiens* hypothetical protein LOC731042 (LOC731042), mRNA.
LIPL4	1.68	PREDICTED: *Homo sapiens* lipase-like, ab-hydrolase domain containing 4 (LIPL4), mRNA.
HS.565086	1.66	UI-H-BI3-alw-d-07-0-UI.s1 NCI_CGAP_Sub5 *Homo sapiens* cDNA clone IMAGE: 30689643, mRNA sequence
UBL4A	1.65	*Homo sapiens* Ubiquitin-Like 4A (UBL4A), mRNA.
CLEC18C	1.64	*Homo sapiens* C-type Lectin Domain Family 18, Member C (CLEC18C), mRNA.
HIST2H2AA3	1.64	*Homo sapiens* Histone Cluster 2, H2aa3 (HIST2H2AA3), mRNA.
UBE2E3	1.63	*Homo sapiens* Ubiquitin-Conjugating Enzyme E2E 3 (UBC4/5 homolog, yeast) (UBE2E3), transcript variant 2, mRNA.
REXO4	1.62	*Homo sapiens* REX4, RNA Exonuclease 4 homolog (S. cerevisiae) (REXO4), mRNA.
HSPE1	1.62	*Homo sapiens* Heat Shock 10kDa protein 1 (chaperonin 10) (HSPE1), mRNA.
SLMO1	1.62	*Homo sapiens* Slowmo homolog 1 (Drosophila) (SLMO1), mRNA.
XPOT	1.61	*Homo sapiens* export in, tRNA (nuclear export receptor for tRNAs) (XPOT), mRNA.
HEATR3	1.60	*Homo sapiens* HEAT repeat containing 3 (HEATR3), mRNA.
HS.61208	1.60	7o98h02.x1 NCI_CGAP_Ov18 *Homo sapiens* cDNA clone IMAGE:3644403 3, mRNA sequence
ODC1	1.59	*Homo sapiens* Ornithine Decarboxylase 1 (ODC1), mRNA.
KIAA1906	1.59	*Homo sapiens* KIAA1906 protein (KIAA1906), mRNA.
SNORD16	1.58	*Homo sapiens* Small Nucleolar RNA, C/D box 16 (SNORD16), small nucleolar RNA.
HS.12764	1.58	*Homo sapiens* cDNA clone IMAGE:5541046, partial cds
HMGA2	1.57	*Homo sapiens* High Mobility Group AT-hook 2 (HMGA2), transcript variant 2, mRNA.
SUFU	1.57	*Homo sapiens* Suppressor of Fused homolog (Drosophila) (SUFU), mRNA.
GRIP2	1.57	*Homo sapiens* Glutamate Receptor Interacting Protein 2 (GRIP2), mRNA.

SDR16C5	1.57	*Homo sapiens* Shortchain Dehydrogenase/Reductase family 16C, member 5 (SDR16C5), mRNA.
LOC729779	1.56	PREDICTED: *Homo sapiens* misc_RNA (LOC729779), misc RNA.
DSCR4	1.56	*Homo sapiens* Down Syndrome Critical Region gene 4 (DSCR4), mRNA.
HS.169815	1.56	op45f10.s1 Soares_NFL_T_GBC_S1 *Homo sapiens* cDNA clone IMAGE:1579819 3, mRNA sequence
GPR176	1.56	*Homo sapiens* G Protein Coupled Receptor 176 (GPR176), mRNA.
HS.438937	1.56	*Homo sapiens* cDNA FLJ41881 fis, clone OCBBF2021833
NQO1	1.55	*Homo sapiens* NAD(P)H dehydrogenase, Quinone 1 (NQO1), transcript variant 1, mRNA.
SLC25A20	1.55	*Homo sapiens* Solute Carrier Family 25 (carnitine/acylcarnitine translocase), member 20 (SLC25A20), nuclear gene encoding mitochondrial protein, mRNA.
BCAR4	1.55	*Homo sapiens* Breast Cancer Anti-Estrogen Resistance 4 (BCAR4), non-coding RNA.
LOC100132106	1.55	PREDICTED: *Homo sapiens* hypothetical protein LOC100132106 (LOC100132106), mRNA.
MIR9-1	1.55	*Homo sapiens* microRNA 9-1 (MIR9-1), microRNA.
SCARNA14	1.54	*Homo sapiens* Small Cajal body-specific RNA 14 (SCARNA14), guide RNA.
HS.378070	1.54	hn28d09.x1 NCI_CGAP_Thy7 *Homo sapiens* cDNA clone IMAGE: 3023441 3, mRNA sequence
TSPAN13	1.54	*Homo sapiens* Tetraspanin 13 (TSPAN13), mRNA.
LOC100129000	1.54	PREDICTED: *Homo sapiens* similar to hCG1647535, transcript variant 1 (LOC100129000), mRNA.
DTNA	1.54	*Homo sapiens* Dystrobrevin, Alpha (DTNA), transcript variant 7, mRNA.
LPPR5	1.54	*Homo sapiens* Lipid Phosphate Phosphatase-Related protein type 5 (LPPR5), transcript variant 1, mRNA.
CD47	-1.54	*Homo sapiens* CD47 molecule (CD47), transcript variant 1, mRNA.
HAS3	-1.54	*Homo sapiens* Hyaluronan Synthase 3 (HAS3), transcript variant 1, mRNA.
ANGPT1	-1.54	*Homo sapiens* Angiopoietin 1 (ANGPT1), mRNA.
IGF1R	-1.54	*Homo sapiens* Insulin-like Growth Factor 1 receptor (IGF1R), mRNA.
TP53INP2	-1.54	*Homo sapiens* Tumor Protein P53 Inducible Nuclear Protein 2 (TP53INP2), mRNA.
CHRNA1	-1.54	*Homo sapiens* Cholinergic Receptor Nicotinic Alpha 1 (muscle) (CHRNA1), transcript variant 1, mRNA.
BNIP3L	-1.54	*Homo sapiens* BCL2/adenovirus E1B 19kDa interacting protein 3 like (BNIP3L), mRNA.
GSN	-1.54	*Homo sapiens* Gelsolin (amyloidosis, Finnish type) (GSN), transcript variant 2, mRNA.
CYB5A	-1.54	*Homo sapiens* Cytochrome b5 type A (microsomal) (CYB5A), transcript variant 2, mRNA.
SP110	-1.54	*Homo sapiens* SP110 nuclear body protein (SP110), transcript variant b, mRNA.
RASGRP3	-1.54	*Homo sapiens* RAS Guanyl Releasing Protein 3 (calcium and DAG-regulated) (RASGRP3), mRNA.
CTGF	-1.54	*Homo sapiens* Connective Tissue Growth Factor (CTGF), mRNA.
RBM39	-1.54	*Homo sapiens* RNA Binding Motif Protein 39 (RBM39), transcript variant 1, mRNA.
DDX60	-1.54	*Homo sapiens* DEAD (Asp-Glu-Ala-Asp) Box Polypeptide 60 (DDX60), mRNA.
MT1F	-1.55	*Homo sapiens* Metallothionein 1F (MT1F), mRNA.
IFIT3	-1.55	*Homo sapiens* Interferon-Induced Protein with Tetratricopeptide repeats 3 (IFIT3), mRNA.
RNF150	-1.55	*Homo sapiens* Ring Finger Protein 150 (RNF150), mRNA.
DNER	-1.55	*Homo sapiens* Delta/Notch-like EGF repeat containing (DNER), mRNA.
LPPR4	-1.55	*Homo sapiens* plasticity related gene 1 (LPPR4), mRNA.
HSD11B1	-1.55	*Homo sapiens* Hydroxysteroid (11-Beta) Dehydrogenase 1 (HSD11B1), transcript variant 1, mRNA.
HECW2	-1.55	*Homo sapiens* HECT, C2 and WW domain containing E3 ubiquitin protein ligase 2 (HECW2), mRNA.
CLEC1A	-1.56	*Homo sapiens* C-Type Lectin Domain Family 1, Member A (CLEC1A), mRNA.
CCRL1	-1.56	*Homo sapiens* Chemokine (C-C Motif) Receptor-Like 1 (CCRL1), transcript variant 2, mRNA.
RARRES1	-1.56	*Homo sapiens* Retinoic Acid Receptor Responder (tazarotene induced) 1 (RARRES1), transcript variant 2, mRNA.
HNMT	-1.56	*Homo sapiens* Histamine N-Methyltransferase (HNMT), transcript variant 2, mRNA.
VPS25	-1.56	*Homo sapiens* Vacuolar Protein Sorting 25 homolog (S. cerevisiae) (VPS25), mRNA.
GAD1	-1.56	*Homo sapiens* Glutamate Decarboxylase 1 (brain, 67kDa) (GAD1), transcript variant GAD25, mRNA.
EIF2AK3	-1.57	*Homo sapiens* Eukaryotic Translation Initiation Factor 2-Alpha Kinase 3 (EIF2AK3), mRNA.
IFIT1	-1.57	*Homo sapiens* Interferon-Induced Protein With Tetratricopeptide Repeats 1 (IFIT1), transcript variant 2, mRNA.
LOC651872	-1.57	PREDICTED: *Homo sapiens* similar to C-C Chemokine Receptor Type 11 (C-C CKR-11) (CC-CKR-11) (CCR-11) (CC Chemokine Receptor-Like 1) (CCRL1) (CCX CKR) (LOC651872), mRNA.
C5ORF41	-1.57	*Homo sapiens* Chromosome 5 open reading frame 41 (C5orf41), mRNA.
C10ORF58	-1.57	*Homo sapiens* Chromosome 10 open reading frame 58 (C10orf58), transcript variant 1, mRNA.

ABLIM1	-1.57	*Homo sapiens* Actin Binding Lim Protein 1 (ABLIM1), transcript variant 4, mRNA.
SSH1	-1.57	*Homo sapiens* Slingshot Homolog 1 (Drosophila) (SSH1), mRNA.
PTK7	-1.57	*Homo sapiens* PTK7 Protein Tyrosine Kinase 7 (PTK7), transcript variant PTK7-4, mRNA.
COL4A2	-1.57	*Homo sapiens* Collagen Type iv Alpha 2 (COL4A2), mRNA.
MESDC1	-1.58	*Homo sapiens* Mesoderm Development Candidate 1 (MESDC1), mRNA.
CDH11	-1.58	*Homo sapiens* Cadherin 11, type 2, OB-cadherin (osteoblast) (CDH11), mRNA.
MAP7	-1.58	*Homo sapiens* Microtubule-Associated Protein 7 (MAP7), mRNA.
PLAC8	-1.58	*Homo sapiens* Placenta-Specific 8 (PLAC8), mRNA.
SYNC1	-1.59	*Homo sapiens* Syncoilin, Intermediate Filament 1 (SYNC1), mRNA.
SMC3	-1.59	*Homo sapiens* Structural Maintenance of Chromosomes 3 (SMC3), mRNA.
CFH	-1.59	*Homo sapiens* Complement Factor H (CFH), transcript variant 1, mRNA.
N4BP2L1	-1.59	*Homo sapiens* NEDD4 binding protein 2-like 1 (N4BP2L1), transcript variant 2, mRNA.
LDHAL6B	-1.59	*Homo sapiens* Lactate Dehydrogenase A-Like 6B (LDHAL6B), mRNA.
GPD2	-1.59	*Homo sapiens* Glycerol-3-Phosphate Dehydrogenase 2 (mitochondrial) (GPD2), nuclear gene encoding mitochondrial protein, transcript variant 1, mRNA.
EID3	-1.59	*Homo sapiens* Ep300 Interacting Inhibitor of Differentiation 3 (EID3), mRNA.
FBLN5	-1.60	*Homo sapiens* Fibulin 5 (FBLN5), mRNA.
NCCRP1	-1.60	*Homo sapiens* Non-Specific Cytotoxic Cell Receptor Protein 1 homolog (zebrafish) (NCCRP1), mRNA.
HGF	-1.60	*Homo sapiens* Hepatocyte Growth Factor (hepapoietin A; scatter factor) (HGF), transcript variant 1, mRNA.
OAS1	-1.60	*Homo sapiens* 2',5'-Oligoadenylate Synthetase 1, 40/46kDa (OAS1), transcript variant 1, mRNA.
KLF4	-1.60	*Homo sapiens* Kruppel Like Factor 4 (gut) (KLF4), mRNA.
SHRM	-1.61	*Homo sapiens* Shroom (SHRM), mRNA.
MAP1LC3A	-1.61	*Homo sapiens* Microtubule-Associated Protein 1 Light Chain 3 Alpha (MAP1LC3A), transcript variant 2, mRNA.
BNIP3L	-1.61	*Homo sapiens* BCL2/Adenovirus E1B 19kDa Interacting Protein 3-Like (BNIP3L), mRNA.
TP53INP1	-1.62	*Homo sapiens* Tumor Protein p53 Inducible Nuclear Protein 1 (TP53INP1), mRNA.
MT1H	-1.62	*Homo sapiens* Metallothionein 1H (MT1H), mRNA.
SIRPA	-1.62	*Homo sapiens* Signal-Regulatory Protein Alpha (SIRPA), transcript variant 3, mRNA.
FILIP1L	-1.62	*Homo sapiens* Filamina Interacting Protein 1-Like (FILIP1L), transcript variant 1, mRNA.
NHS	-1.62	*Homo sapiens* Nance-Horan Syndrome (congenital cataracts and dental anomalies) (NHS), transcript variant 1, mRNA.
LYPD1	-1.62	*Homo sapiens* LY6/PLAUR Domain containing 1 (LYPD1), transcript variant 1, mRNA.
KIF11	-1.63	*Homo sapiens* Kinesin Family Member 11 (KIF11), mRNA.
CEACAM1	-1.63	*Homo sapiens* Carcinoembryonic Antigen-Related Cell Adhesion Molecule 1 (biliary glycoprotein) (CEACAM1), transcript variant 2, mRNA.
FAM43A	-1.63	*Homo sapiens* Family with sequence similarity 43, member A (FAM43A), mRNA.
NUAK2	-1.63	*Homo sapiens* NUAK family, snf1-like kinase, 2 (NUAK2), mRNA.
GPD2	-1.63	*Homo sapiens* Glycerol-3-Phosphate Dehydrogenase 2 (mitochondrial) (GPD2), mRNA.
CYP24A1	-1.63	*Homo sapiens* Cytochrome P450, family 24, subfamily A, Polypeptide 1 (CYP24A1), nuclear gene encoding mitochondrial protein, mRNA.
HLA-DPA1	-1.64	*Homo sapiens* major Histocompatibility complex, class II, DP Alpha 1 (HLA-DPA1), mRNA.
ABI3BP	-1.65	*Homo sapiens* ABI gene family, member 3 (NESH) binding protein (ABI3BP), mRNA.
USP18	-1.65	*Homo sapiens* Ubiquitin Specific Peptidase 18 (USP18), mRNA.
FABP3	-1.65	*Homo sapiens* Fatty Acid Binding Protein 3, muscle and heart (mammary-derived growth inhibitor) (FABP3), mRNA.
KCNK2	-1.65	*Homo sapiens* Potassium Channel, subfamily K, member 2 (KCNK2), transcript variant 3, mRNA.
CYP51A1	-1.66	*Homo sapiens* Cytochrome P450, family 51, subfamily A, polypeptide 1 (CYP51A1), mRNA.
CYP1B1	-1.66	*Homo sapiens* Cytochrome P450, family 1, subfamily B, Polypeptide 1 (CYP1B1), mRNA.
PLAT	-1.66	*Homo sapiens* Plasminogen Activator, Tissue (PLAT), transcript variant 1, mRNA.
HLA-DRB6	-1.66	*Homo sapiens* major Histocompatibility complex, class II, DR beta 6 (pseudogene) (HLA-DRB6), non-coding RNA.
LOC100131093	-1.67	PREDICTED: *Homo sapiens* misc_RNA (LOC100131093), miscRNA.
FBLN5	-1.67	*Homo sapiens* Fibulin 5 (FBLN5), mRNA.
MUC1	-1.67	*Homo sapiens* Mucin 1, cell surface associated (MUC1), transcript variant 5, mRNA.
SEMA3C	-1.67	*Homo sapiens* SEMA domain, Immunoglobulin domain (Ig), short basic domain, secreted, (Semaphorin) 3C (SEMA3C), mRNA.

NNMT	-1.67	*Homo sapiens* Nicotinamide N-Methyltransferase (NNMT), mRNA.
TNFSF13B	-1.68	*Homo sapiens* Tumor Necrosis factor (ligand) superfamily, member 13b (TNFSF13B), transcript variant 1, mRNA.
FAM20A	-1.68	*Homo sapiens* Family with sequence similarity 20, member A (FAM20A), mRNA.
FBXO32	-1.68	*Homo sapiens* F-Box Protein 32 (FBXO32), transcript variant 2, mRNA.
EDNRA	-1.68	*Homo sapiens* Endothelin Receptor Type A (EDNRA), mRNA.
CFB	-1.68	*Homo sapiens* Complement Factor B (CFB), mRNA.
ADAMDEC1	-1.68	*Homo sapiens* ADAM-Like, Decysin 1 (ADAMDEC1), mRNA.
HS.561679	-1.68	DA830074 PLACE1 *Homo sapiens* cDNA clone PLACE1004374 5, mRNA sequence
PALLD	-1.68	*Homo sapiens* Palladin, cytoskeletal associated protein (PALLD), transcript variant 2, mRNA.
EGFL6	-1.69	*Homo sapiens* EGF-Like-Domain, Multiple 6 (EGFL6), mRNA.
LRRN3	-1.69	*Homo sapiens* Leucine Rich Repeat neuronal 3 (LRRN3), transcript variant 1, mRNA.
FILIP1L	-1.70	*Homo sapiens* Filamina Interacting Protein 1-Like (FILIP1L), transcript variant 2, mRNA.
SEPT4	-1.70	*Homo sapiens* Septin 4 (SEPT4), transcript variant 1, mRNA.
C9ORF135	-1.70	*Homo sapiens* Chromosome 9 open reading frame 135 (C9orf135), mRNA.
HLA-DRB5	-1.70	*Homo sapiens* major Histocompatibility complex, class II, DR Beta 5 (HLA-DRB5), mRNA.
TFPI2	-1.71	*Homo sapiens* Tissue Factor Pathway inhibitor 2 (TFPI2), mRNA.
CYB5A	-1.72	*Homo sapiens* cytochrome b5 type A (microsomal) (CYB5A), transcript variant 2, mRNA.
ARHGAP28	-1.73	*Homo sapiens* Rho GTPase activating protein 28 (ARHGAP28), transcript variant 1, mRNA.
LRDD	-1.73	*Homo sapiens* Leucine-Rich Repeats and Death Domain containing (LRDD), transcript variant 2, mRNA.
SLC26A4	-1.74	*Homo sapiens* Solute carrier family 26, member 4 (SLC26A4), mRNA.
MT1JP	-1.74	*Homo sapiens* Metallothionein 1J (pseudogene) (MT1JP), mRNA.
VCAN	-1.75	*Homo sapiens* Versican (VCAN), mRNA.
C13ORF15	-1.76	*Homo sapiens* Chromosome 13 open reading frame 15 (C13orf15), mRNA.
NR4A2	-1.76	*Homo sapiens* Nuclear Receptor subfamily 4, group A, member 2 (NR4A2), transcript variant 1, mRNA.
SEPT4	-1.77	*Homo sapiens* Septin 4 (SEPT4), transcript variant 3, mRNA.
THBS2	-1.79	*Homo sapiens* Thrombospondin 2 (THBS2), mRNA.
IL4I1	-1.79	*Homo sapiens* Interleukin 4 Induced 1 (IL4I1), transcript variant 2, mRNA.
TNFSF13B	-1.80	*Homo sapiens* Tumor Necrosis Factor (ligand) superfamily, member 13b (TNFSF13B), transcript variant 1, mRNA.
MASP1	-1.80	*Homo sapiens* Mannan-Binding Lectin Serine Peptidase 1 (C4/C2 activating component of Ra-reactive factor) (MASP1), transcript variant 2, mRNA.
RASL11B	-1.81	*Homo sapiens* RAS-Like, family 11, member B (RASL11B), mRNA.
LRRN3	-1.81	*Homo sapiens* Leucine Rich Repeat Neuronal 3 (LRRN3), mRNA.
CLDN1	-1.81	*Homo sapiens* Claudin 1 (CLDN1), mRNA.
SLC39A8	-1.81	*Homo sapiens* Solute carrier family 39 (zinc transporter), member 8 (SLC39A8), transcript variant 1, mRNA.
FLJ21986	-1.81	*Homo sapiens* hypothetical protein FLJ21986 (FLJ21986), mRNA.
PSTPIP2	-1.83	*Homo sapiens* Proline-Serine-Threonine Phosphatase Interacting Protein 2 (PSTPIP2), mRNA.
SEPT4	-1.83	*Homo sapiens* Septin 4 (SEPT4), transcript variant 2, mRNA.
LOC100134073	-1.84	PREDICTED: *Homo sapiens* similar to LYPDC1 protein (LOC100134073), mRNA.
SLC2A5	-1.85	*Homo sapiens* Solute carrier family 2 (facilitated glucose/fructose transporter), member 5 (SLC2A5), mRNA.
CCL5	-1.87	*Homo sapiens* Chemokine (C-C motif) Ligand 5 (CCL5), mRNA.
STX11	-1.87	*Homo sapiens* Syntaxin 11 (STX11), mRNA.
HLA-DRB4	-1.87	*Homo sapiens* Major Histocompatibility complex, class II, DR Beta 4 (HLA-DRB4), mRNA.
LOC649143	-1.89	PREDICTED: *Homo sapiens* similar to HLA class II histocompatibility antigen, DRB1-9 beta chain precursor (MHC class I antigen DRB1*9) (DR-9) (DR9), transcript variant 2 (LOC649143), mRNA.
NR4A2	-1.89	*Homo sapiens* Nuclear Receptor Subfamily 4, group A, member 2 (NR4A2), transcript variant 1, mRNA.
SLC39A8	-1.90	*Homo sapiens* Solute Carrier Family 39 (zinc transporter), member 8 (SLC39A8), transcript variant 1, mRNA.
HLA-DRB6	-1.90	*Homo sapiens* Major Histocompatibility Complex, class II, DR beta 6 (pseudogene) (HLA-DRB6), non-coding RNA.
CXCL11	-1.92	*Homo sapiens* Chemokine (C-X-C motif) Ligand 11 (CXCL11), mRNA.
IFIT2	-1.92	*Homo sapiens* Interferon-Induced Protein with Tetratricopeptide Repeats 2 (IFIT2), mRNA.
MUC1	-1.93	*Homo sapiens* Mucin 1, cell surface associated (MUC1), transcript variant 6, mRNA.
LIPG	-1.97	*Homo sapiens* Lipase, endothelial (LIPG), mRNA.

SULF1	-1.98	*Homo sapiens* Sulfatase 1 (SULF1), mRNA.
UBD	-2.03	*Homo sapiens* Ubiquitin D (UBD), mRNA.
XIRP1	-2.04	*Homo sapiens* Xin actin-binding repeat containing 1 (XIRP1), mRNA.
HLA-DRA	-2.06	*Homo sapiens* Major Histocompatibility Complex, class II, DR Alpha (HLA-DRA), mRNA.
CD74	-2.07	*Homo sapiens* CD74 molecule, major histocompatibility complex, class II invariant chain (CD74), transcript variant 1, mRNA.
CD74	-2.08	*Homo sapiens* CD74 molecule, major histocompatibility complex, class II invariant chain (CD74), transcript variant 2, mRNA.
TNFSF10	-2.10	*Homo sapiens* Tumor Necrosis Factor (ligand) superfamily, member 10 (TNFSF10), mRNA.
HAS3	-2.10	*Homo sapiens* Hyaluronan Synthase 3 (HAS3), transcript variant 1, mRNA.
LOC730415	-2.12	PREDICTED: *Homo sapiens* hypothetical LOC730415, transcript variant 2 (LOC730415), mRNA.
A2M	-2.12	*Homo sapiens* Alpha-2-Macroglobulin (A2M), mRNA.
IGFBP5	-2.15	*Homo sapiens* Insulin-Like Growth Factor Binding Protein 5 (IGFBP5), mRNA.
HLA-DRA	-2.21	*Homo sapiens* Major Histocompatibility Complex, class II, DR alpha (HLA-DRA), mRNA.
CX3CL1	-2.28	*Homo sapiens* Chemokine (C-X3-C motif) ligand 1 (CX3CL1), mRNA.
HLA-DRB1	-2.28	*Homo sapiens* Major Histocompatibility Complex, class II, DR beta 1 (HLA-DRB1), mRNA.
CCL5	-2.32	*Homo sapiens* Chemokine (C-C motif) ligand 5 (CCL5), mRNA.
PEG10	-2.33	PREDICTED: *Homo sapiens* Paternally Expressed 10 (PEG10), mRNA.
VCAM1	-2.35	*Homo sapiens* Vascular Cell Adhesion Molecule 1 (VCAM1), transcript variant 1, mRNA.
VCAM1	-2.51	*Homo sapiens* Vascular Cell Adhesion Molecule 1 (VCAM1), transcript variant 1, mRNA.
METTL7A	-3.12	*Homo sapiens* Methyltransferase like 7A (METTL7A), mRNA.

Table 2: The 200 genes most modulated by spearmint essential oil (SEO, 0.011% v/v) (in $\log_2$ relative ratio form).

Gene Symbol	Entrez Gene Name	Illumina Probe ID	Location	Protein Type	Entrez Gene ID for Human	Fold Change Over Vehicle
KLF6	Kruppel-Like Factor 6	ILMN_1700727	Nucleus	Transcription Regulator	1316	1.535
COL10A1	Collagen, type X, alpha 1	ILMN_1672776	Extracellular Space	Other	1300	1.493
IL6R	Interleukin 6 Receptor	ILMN_1754753	Plasma Membrane	Transmembrane Receptor	3570	1.394
COL6A3	Collagen, type VI, alpha 3	ILMN_2307861	Extracellular Space	Other	1293	-1.405
MMP2	Matrix Metallopeptidase 2	ILMN_1762106	Extracellular Space	Peptidase	4313	-1.405
NFKB2	Nuclear Factor of Kappa Light Polypeptide Gene Enhancer in B-cells 2 (P49/pIOO)	ILMN_1799062	Nucleus	Transcription Regulator	4791	1.408
MYH11	Myosin, Heavy Chain 11, Smooth Muscle	ILMN_1660086	Cytoplasm	Other	4629	-1.437
COL11A1	Collagen, Type XI, alpha 1	ILMN_1789507	Extracellular Space	Other	1301	-1.453
COL4A1	Collagen, Type IV, alpha 1	ILMN_1653028	Extracellular Space	Other	1282	-1.503
MYH10	Myosin, Heavy Chain 10, Non-Muscle	ILMN_1815154	Cytoplasm	Other	4628	-1.506
CXCL9	Chemokine (C-X-C motif) Ligand 9	ILMN_1745356	Extracellular Space	Cytokine	4283	-1.524
IGF1R	Insulin-Like Growth Factor 1 Receptor	ILMN_1675048	Plasma Membrane	Transmembrane Receptor	3480	-1.537
CTGF	Connective tissue growth factor	ILMN_2115125	Extracellular Space	Growth Factor	1490	-1.543
COL4A2	Collagen, Type IV. alpha 2	ILMN_1724994	Extracellular Space	Other	1284	1.574
HGF	Hepatocyte Growth Factor (Hepapoietin A; Scatter Factor)	ILMN_1801586	Extracellular Space	Growth Factor	3082	1.601
EDNRA	Endothelin Receptor Type A	ILMN_1796629	Plasma Membrane	Transmembrane Receptor	1909	-1.678
A2M	Alpha-2-Macroglobulin	ILMN_1745607	Extracellular Space	Transporter	2	-2.125
IGFBP5	Insulin-Like Growth Factor Binding Protein 5	ILMN_2132982	Extracellular Space	Other	3488	-2.147
CCL5	Chemokine (C-C motif) Ligand 5	ILMN_1773352	Extracellular Space	Cytokine	6352	-2.322
VCAM1	Vascular Cell Adhesion Molecule 1	ILMN_1766955	Plasma Membrane	Transmembrane Receptor	7412	-2.512

Table 3: Top 20 genes regulated by Spearmint Essential Oil (SEO, 0.011% v/v) in the canonical hepatic fibrosis/hepatic stellate cell activation pathway. Fold change over vehicle was shown in $\log_2$ ratio form.

Gene Symbol	Entrez Gene Name	Illumina Probe ID	Location	Protein Type	Entrez Gene ID for Human	Fold Change Over Vehicle
MR1	Major Histocompatibility Complex, Class I-related	ILMN 2167416	Plasma Membrane	Transmembrane receptor	3140	-1.261
HLA-DMB	Major Histocompatibility Complex, Class II, DM Beta	ILMN_1761733	Plasma Membrane	Transmembrane receptor	3109	-1.307
HLA-C	Major Histocompatibility Complex, Class 1, C	ILMN_2150787	Plasma Membrane	other	3107	-1.316
HLA-G	Major Histocompatibility Complex, Class 1, G	ILMN_1656670	Plasma Membrane	other	3135	-1.341
HLA-B	Major Histocompatibility Complex, Class 1, B	ILMN 1778401	Plasma Membrane	Transmembrane receptor	3106	-1.368
HLA-DRB3	Major Histocompatibility Complex, Class II, DR Beta 3	ILMN 1717261	Cytoplasm	other	3125	-1.381
HLA-DQA1	Major Histocompatibility Complex, Class II, DQ alpha 1	ILMN_1808405	Plasma Membrane	Transmembrane receptor	3117	-1.401
TAPBP	TAP Binding Protein (tapasin)	ILMN_1742450	Cytoplasm	Transporter	6892	-1.475
HLA-F	Major Histocompatibility Complex, Class 1, F	ILMN_1762861	Plasma Membrane	Transmembrane receptor	3134	-1.521
HLA-DPA1	Major Histocompatibility Complex, Class II, DP Alpha 1	ILMN 1772218	Plasma Membrane	Transmembrane receptor	3113	-1.641
HLA-DRB5	Major Histocompatibility Complex, Class II, DR Beta 5	ILMN 1697499	Plasma Membrane	Transmembrane receptor	3127	-1.704
HLA-DRB4	Major Histocompatibility Complex, Class II, DR Beta 4	ILMN_1752592	Plasma Membrane	Transmembrane receptor	3126	-1.869
CD74	CD74 molecule, Major Histocompatibility Complex, Class II invariant chain	ILMN 2379644	Plasma Membrane	Transmembrane receptor	972	-2.079
HLA-DRA	Major Histocompatibility Complex, Class II, DR Alpha	ILMN 2157441	Plasma Membrane	Transmembrane receptor	3122	-2.212
HLA-DRB1	Major Histocompatibility Complex, Class II, DR Beta 1	ILMN_1715169	Plasma Membrane	Transmembrane receptor	3123	-2.279

Table 4: Top 15 genes regulated by Spearmint Essential Oil (SEO, 0.011% v/v) in the canonical antigen presentation pathway. Fold change over vehicle was shown in $\log_2$ ratio form.

Gene Symbol	Entrez Gene Name	Illumina Probe ID	Location	Protein Type	Entrez Gene ID for Human	Fold Change Over Vehicle
IL37	Interleukin 37	ILMN 1697710	Extracellular Space	cytokine	27178	1.313
IL36RN	Interleukin 36 Receptor Antagonist	ILMN_1759141	Extracellular Space	cytokine	26525	-1.262
IL1RN	Interleukin 1 Receptor Antagonist	ILMN 1689734	Extracellular Space	cytokine	3557	-1.269
TNF	Tumor Necrosis Factor	ILMN_1728106	Extracellular Space	cytokine	7124	-1.273
HLA-DMB	Major Histocompatibility Complex, Class II, DM Beta	ILMN 1761733	Plasma Membrane	transmembrane receptor	3109	-1.307
HLA-C	Major Histocompatibility Complex, class 1, C	ILMN 2150787	Plasma Membrane	other	3107	-1.316
HLA-G	Major Histocompatibility Complex, class 1, G	ILMN_1656670	Plasma Membrane	other	3135	-1.341
HLA-B	Major Histocompatibility Complex, class 1, B	ILMN 1778401	Plasma Membrane	transmembrane receptor	3106	-1.368
IL33	Interleukin 33	ILMN 1809099	Extracellular Space	cytokine	90865	-1.382
FAS	FAS cell surface death receptor	ILMN 2319077	Plasma Membrane	transmembrane receptor	355	-1.392
HLA-DQA1	Major Histocompatibility Complex, class II, DQ Alpha 1	ILMN_1808405	Plasma Membrane	transmembrane receptor	3117	-1.401
HLA-F	Major Histocompatibility Complex, class 1, F	ILMN_1762861	Plasma Membrane	transmembrane receptor	3134	-1.521
HLA-DRB5	Major Histocompatibility Complex, class II, DR Beta 5	ILMN 1697499	Plasma Membrane	transmembrane receptor	3127	-1.704
HLA-DRA	Major Histocompatibility Complex, class II, DR Alpha	ILMN 2157441	Plasma Membrane	transmembrane receptor	3122	-2.212
HLA-DRB1	Major Histocompatibility Complex, class II, DR Beta 1	ILMN_1715169	Plasma Membrane	transmembrane receptor	3123	-2.279

Table 5: Top 15 genes regulated by Spearmint Essential Oil (SEO, 0.011% v/v) in the canonical graft-versus-host disease signaling pathway. Fold change over vehicle was shown in $\log_2$ ratio form.

Gene Symbol	Entrez Gene Name	Illumina Probe ID	Location	Protein Type	Entrez Gene ID for Human	Fold Change Over Vehicle
TNF	Tumor Necrosis Factor	IIMN_1728106	Extracellular Space	cytokine	7124	-1.273
HLA-DMB	Major Histocompatibility Complex, Class II, DM Beta	ILMN_1761733	Plasma Membrane	Transmembrane Receptor	3109	-1.307
HLA-C	Major Histocompatibility Complex, Class 1, C	IIMN_2150787	Plasma Membrane	Other	3107	-1.316
HLA-G	Major Histocompatibility Complex, Class 1, G	IIMN_1656670	Plasma Membrane	Other	3135	-1341
HLA-B	Major Histocompatibility Complex, Class 1. B	IIMN_1778401	Plasma Membrane	Transmembrane Receptor	3106	-1.368
HLA-DRB3	Major Histocompatibility Complex, Class II, DR Beta 3	ILMN 1717261	Cytoplasm	Other	3125	-1.381
FAS	FAS Cell Surface Death Receptor	ILMN_2319077	Plasma Membrane	Transmembrane Receptor	355	-1.392
HLA-DQA1	Major Histocompatibility Complex, Class II, DQ Alpha 1	IIMN_1808405	Plasma Membrane	Transmembrane Receptor	3117	-1.401
HLA-F	Major Histocompatibility Complex, Class 1, F	ILMN_1762861	Plasma Membrane	Transmembrane Receptor	3134	-1.521
HLA-DPA1	Major Histocompatibility Complex, Class II, DP Alpha 1	ILMN_1772218	Plasma Membrane	Transmembrane Receptor	3113	-1.641
HLA-DRB5	Major Histocompatibility Complex, Class II, DR Beta 5	ILMN 1697499	Plasma Membrane	Transmembrane Receptor	3127	-1 704
HLA-DRB4	Major Histocompatibility Complex, Class II. DR Beta 4	ILMN_1752592	Plasma Membrane	Transmembrane Receptor	3126	-1.869
HLA-DRA	Major Histocompatibility Complex, Class II. OR Alpha	ILMN_2157441	Plasma Membrane	Transmembrane Receptor	3122	-2.212
HLA-DRB1	Major Histocompatibility Complex, Class II, DR Beta 1	ILMN_1715169	Plasma Membrane	Transmembrane Receptor	3123	-2.279

Table 6: Top 14 genes regulated by Spearmint Essential Oil (SEO, 0.011% v/v) in the canonical allograft rejection signaling pathway. Fold change over vehicle was shown in $\log_2$ ratio form.